Inorg. Chem. **2004**, *43*, 8301–8309

Multiple Pathways for the Oxygenation of a Ruthenium(II) Dithiocarbamate Complex: S-Oxygenation and S-Extrusion

Szeman Ng, Joseph W. Ziller, and Patrick J. Farmer*

Department of Chemistry, University of California, Irvine, California 92697-2025

Received September 23, 2004

The reactions of Ru(bpy)$_2$(*N*,*N*-dimethyldithiocarbamate)$^+$, **1**, with O-atom-transfer reagents such as hydrogen peroxide, *m*-chloroperoxybenzoic acid, and oxone have been studied and several resulting derivatives isolated and structurally characterized. Both S-oxygenation and S-extrusion may occur depending upon reagent and conditions. Excess peroxygenation leads to a stable dioxygenate, Ru(bpy)$_2$(*N*,*N*-dimethylthiocarbamatesulfinate-*S*,*S*)$^+$, **3**. Stoichiometric oxygenation leads to mixtures of products from which two forms of monooxygenated species Ru(bpy)$_2$(*N*,*N*-dimethylperoxydithiocarbamate-*S*,*S*), **2a**, and Ru(bpy)$_2$(*N*,*N*-dimethylperoxydithiocarbamate-*O*,*S*), **2b**, and an S-extruded product, Ru(bpy)$_2$(*N*,*N*-dimethylmonothiocarbamate)$^+$, **4**, have been isolated as PF_6^- salts. The S,S-bound monooxygenate is unstable over time toward either O-atom-transfer reactions via disproportionation or reaction with phosphines or S-extrusion yielding complex **4** in which the thiocarbamate is bonded solely through the remaining S atom. All the complexes have been characterized by ^{1}H NMR, UV–vis, and mass spectroscopies, and all but the highly reactive **2a** structurally determined by X-ray crystallography.

Introduction

Metal complexes and derivatives of dithiocarbamates (DTCs) have long been used as vulcanizing agents,[1] pesticides,[2] and drugs.[3] Certain aspects of the biological activity of these compounds have been proposed to depend on in vivo S-oxygenation,[4−6] which leads to S-extruded products. For instance, various S-oxygenated and S-extruded derivatives have been shown to have higher activity against known targets such as aldehyde dehydrogenase. The chemical pathway of oxidative S-extrusion has been best characterized in vitro, Scheme 1.[7] The peroxidation of S-alkylated dialkyldithiocarbamates affords a sulfine intermediate that is isolable at low temperatures, but at room temperature the compound extrudes sulfur, via a purported oxathiirane intermediate, to form the S-alkylated monothiocarbamate (MTC). In search of a common pathway for neurotoxicity, a recent EPA report on DTC pesticides states that the "formation of a reactive sulfoxide metabolite is a plausible common critical event" that may be associated with side effects of exposure.[8]

Scheme 1

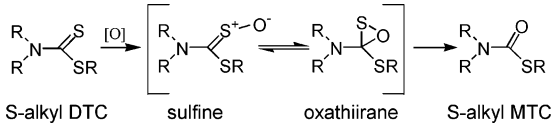

Our interest follows from recent reports that DTC salts induce an apoptotic response in a variety of cell lines, attributed to metal uptake and the resulting intracellular oxidative stress.[9,10] We have shown that Cu and Zn DTC compounds have selective toxicity toward melanoma cancer[11] and that similar activity of disulfiram, a disulfide DTC derivative, is Cu dependent.[12] As much of the biological activity of *S*-alkyl DTC compounds are suggested to be via

* Author to whom correspondence should be addresed. E-mail: pfarmer@uci.edu.

(1) Nieuwenhuizen, P. J.; Timal, S.; Haasnoot, J. G.; Spek, A. L.; Reedijk, J. *Chem. Eur. J.* **1997**, *3*, 1846−1851.
(2) Malike, A. K.; Faubel, W. *Pestic. Sci.* **1999**, *55*, 965−970.
(3) Brewer, C. *Alcohol Alcohol. (Oxford)* **1993**, *28*, 383−395.
(4) Madan, A.; Faiman, M. D. *Drug Metab. Dispos.* **1994**, *22*, 324−330.
(5) Madan, A.; Faiman, M. D. *J. Pharmacol. Exp. Ther.* **1995**, *272*, 775−780.
(6) Hu, P.; Jin, L.; Baillie, T. A. *J. Pharmacol. Exp. Ther.* **1997**, *281*, 611−617.
(7) Chevrie, D.; Metzner, P. *Tetrahedron Lett.* **1998**, *39*, 8983−8986.
(8) *The Determination of Whether Dithiocarbamate Pesticides Share a Common Mechanism of Toxicity*; Health Effects Division; Office of Pesticide Programs; U.S. Environmental Protection Agency: Washington, DC, 2001.
(9) Erl, W.; Weber, C.; Hansson, G. K. *Am. J. Physiol.* **2000**, *278*, C1116−C1125.
(10) (a) Nobel, C. S. I.; Kimland, M.; Lind, B.; Orrenius, S.; Slater, A. F. G. *J. Biol. Chem.* **1995**, *270*, 26202−26208. (b) Orrenius, S.; Nobel, C. S. I.; Bandendobbelsteen, D. J.; Burkitt, M. J.; Slater, A. F. G. *Biochem. Soc. Trans.* **1996**, *24*, 1032−1038.
(11) Farmer, P. J.; Gidanian, S.; Shahandeh, B.; Di Bilio, A. J.; Tohidian, N.; Meyskens, F. L., Jr. *Pigm. Cell Res.* **2003**, *16*, 273−279.

10.1021/ic048661a CCC: $27.50
Published on Web 11/25/2004

Chart 1

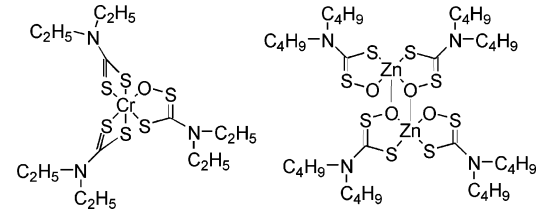

$Cr(S_2CN(C_2H_5)_2)_2(OS_2CN(C_2H_5)_2)$ $[Zn(OS_2CN(C_4H_9)_2]_2$

S-oxygenation and S-extrusion, we postulated that reactivity similar to that of Scheme 1 may occur upon oxygenation of DTC complexes with transition metals and thus be a possible route of xenobiotic activation for widely used DTC pesticides.[8]

Isolable sulfenate products from the monooxygenation of a metal-bound thiolates are somewhat rare,[13−21] but recently a number of such complexes have been isolated and crystallographically characterized as models for the metalloenzyme nitrile hydratase.[22,23] The cumulative literature suggests that metal-bound sulfenates are not inherently unstable but are typically subject to further reactions under conditions of their formation. Likewise, few examples of metal-bound S-oxygenated DTCs are known. The peroxidation of the sodium salt of deDTC yields an *S*-oxide derivative which can be isolated at low temperature;[7] upon warming and decomposition, both disulfide and MTC products are formed. It has also been shown that the S-oxygenated form precedes disulfide formation during the reaction of peroxide with simple DTC salts.[24] The first crystal structure of a metalloperoxydithiocarbamate was obtained from reaction of the sodium salt of *N*,*N*-dimethyldithiocarbamate, Na(mDTC), with $K_2Cr_2O_7$ which yielded a Cr(mDTC)$_2$(O-mDTC) compound with one "dithioperoxycarbamate" ligand, Chart 1.[25,26] Here, the S-oxygenation results

Chart 2 [a]

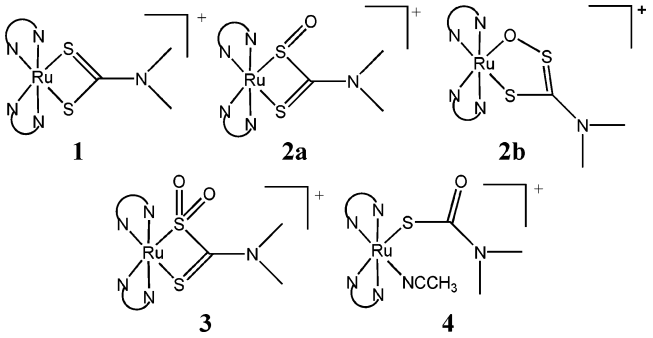

[a] N−N = bpy.

in a ring expansion of the metal−ligand chelate from a four- to a five-membered ring. A similar oxygenated DTC adduct was thought to be generated by reaction of Co(en)$_2$(mDTC)$^+$ with peroxide, though the product was not well characterized.[27,28] Also shown in Chart 1 is a Zn peroxydithiocarbamate recently characterized.[29] Numerous examples exist of analogous "perthio" DTC complexes, which result from insertion of an S-atom into the M−SCS− metallocycle.[30]

While the coordination chemistry of dithiocarbamates has been extensively studied, no systematic study of the oxygenation of these compounds has been performed. With the objective of isolating and characterizing S-oxygenated derivatives, we targeted a kinetically inert Ru(II) mono-DTC complex for reaction studies. Monooxygenated forms of several Ru−thiolate complexes have been observed as kinetic products from reaction with oxone but not isolated.[31] In one recent study, tris(*N*,*N*-diethyldithiocarbamato) complexes of ruthenium(III) were shown to undergo predominantly ligand-based oxidation, though no ligand-oxidized products were isolated.[32] Here, we report the synthesis of the monocationic complex bis(bipyridyl)(*N*,*N*-dimethyldithiocarbamato)ruthenium(II), Ru(bpy)$_2$(dmDTC)$^+$ or **1**, and show that its reaction with O-atom-transfer agents does yield a series of isolable metal complexes, including two linkage isomers of monooxygenates (**2a**,**b**), a dioxygenate (**3**), and a monothiocarbamate from the extrusion of S from the dmDTC (**4**), illustrated in Chart 2.

Results and Discussion

Ru(bpy)$_2$(dmDTC)$^+$ as a Reactivity Model. Ru(bpy)$_2$(dmDTC)$^+$ (dmDTC: dimethyldithiocarbamate or **1**) was readily prepared from the reaction of Na(dmDTC) with Ru(bpy)$_2$(Cl)$_2$ and isolated as the air-stable PF_6 salt. Purified **1** is darkish red, diamagnetic, and highly soluble in polar organic solvents. As will be described below, reactions of **1** with O-atom-transfer reagents allowed identification of different oxygenation pathways leading to S-oxygenated and S-extruded products.

(12) Cen, D.; Brayton, D.; Shahandeh, B.; Meyskens, F. L.; Farmer, P. J., in press, *J. Med. Chem.*
(13) Farmer, P. J.; Verpeaux, J.-N.; Amatore, C.; Darensbourg, M. Y.; Musie, G. *J. Am. Chem. Soc.* **1994**, *116*, 9355−9356.
(14) Sargeson, A. M.; Gainsford, G. J.; Jackson, W. G. *J. Am. Chem. Soc.* **1982**, *104*, 137−141.
(15) Deutsch, E.; Adzamli, I. K.; Libson, K.; Lydon, J. D.; Elder, R. C. *Inorg. Chem.* **1979**, *18*, 303−311.
(16) Darensbourg, M. Y.; Font, I.; Buonomo, R.; Reibenspies, J. H. *Inorg. Chem.* **1993**, *32*, 5897−5898.
(17) Darensbourg, M. Y.; Buonomo, R. M.; Font, I.; Maguire, M. J.; Reibenspies, J. H.; Tuntulani, T. *J. Am. Chem. Soc.* **1995**, *117*, 963−973.
(18) Weigand, W.; Wunsch, R.; Bosl, G.; Robl, C. *J. Organomet. Chem.* **2001**, *621*, 352−358.
(19) Kojima, M.; Murata, M.; Hioki, A.; Miyagawa, M.; Hirotsu, M.; Nakajima, K.; Kita, M.; Kashino, S.; Yoshikawa, Y. *Coord. Chem. Rev.* **1998**, *174*, 109−131.
(20) Shiu, K. B.; Chen, J. Y.; Yu, S. J.; Wang, S. L.; Liao, F. L.; Wang, Y.; Lee, G. H. *J. Organomet. Chem.* **2002**, *648*, 193−203.
(21) Jackson, W. G.; Rahman, A. F. M. M.; Craig, D. C. *Inorg. Chem.* **2003**, *42*, 383−388.
(22) Chottard, J.-C.; Heinrich, L.; Li, Y.; Vaissermann, J. *Eur. J. Inorg. Chem.* **2001**, 1407−1409.
(23) Kovacs, J. A.; Kung, I.; Schweitzer, D.; Shearer, J.; Taylor, W. D.; Jackson, H. L.; Lovell, S. *J. Am. Chem. Soc.* **2000**, *122*, 8299−8300.
(24) Ishimura, Y.; Watanabe, Y. *J. Org. Chem.* **1988**, *53*, 2119−2120.
(25) Martin, R. L.; Hope, J. M.; Taylor, D. *Chem. Commun.* **1977**, *3*, 99−100.
(26) Martin, R. L.; Patrick, J. M.; Skelton, B. W.; Taylor, D.; White, A. H. *Aust. J. Chem.* **1982**, *35*, 2551−1556.
(27) Kita, M.; Yamanari, K.; Shimura, Y. *Chemistry Lett.* **1984**, 297−300.
(28) Kita, M.; Yamanari, K.; Shimara, Y. *Bull. Chem. Soc. Jpn.* **1989**, *62*, 23−32.
(29) Reck, G.; Becker, R.; Walther, G. *Z. Kristallogr.* **1995**, *210*, 769−774.
(30) Coucouvanis, D. *Prog. Inorg. Chem.* **1979**, *26*, 301−469.
(31) Johnson, M. D.; Nickerson, D. *Inorg. Chem.* **1992**, *31*, 3971−4.
(32) Pignolet L. H.; Mattson, B. M.; Heiman, J. R. *Inorg. Chem.* **1976**, *15*, 564−571.

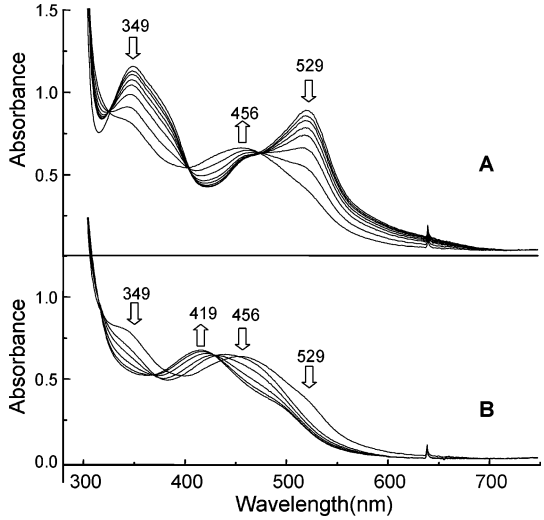

Figure 1. Sequential electronic absorbance spectra of reaction of **1** with 100-fold excess H_2O_2 in CH_3OH at room temperature: (A) changes over initial 13 min, (B) changes over next 20 min. The final spectrum is similar to that of the dioxygenate, **3**.

Oxygenation Reactions of 1. In the methanol, **1** is unreactive toward stoichiometric hydrogen peroxide over 1 day but does react slowly with excess peroxide to yield the dioxygenated complex **3**, as illustrated in Figure 1. During the initial period of this reaction, the two isosbestic points in the spectra imply an apparent conversion to an intermediate species, presumably a monooxygenated form. During the subsequent period, the isosbestic points are lost and a mixture of products results; the final spectrum resembled that of the dioxygenate, **3**, but under these conditions the spectra continues to degrade over time. To isolate products from these reactions, dimethyl sulfide (DMS) was added to quench the excess of peroxide and column separation yielded **3** in greater than 50% yield. Lowering the pH by addition of HCl or HOTf during the reactions with peroxide increased the rate of reaction but gave lower yields of **3**. The reaction of **1** with stoichiometric oxone (the potassium salt of peroxysulfate, K_2SO_5) also directly yielded the dioxygenate **3**, but isolable yields were below 30%.

In the methanol, the reaction of **1** with *meta*-chloroperbenzoic acid, mCPBA, is slow but gives an initial product of single O-atom addition, as characterized by a $[M + 16]^+$ ion in the ESI-MS (Supporting Information, Figure S1a). In contrast, the reaction of **1** with a stoichiometric mCPBA in CH_3CN gave a complex product mixture that was separated by chromatography. Greater than 70% **1** was recovered; the main product (ca. 50% of the reacted **1**) was isolated as an orange species whose isotope pattern fits that of a Ru-bound monothiocarbamate, **4**, formed by S-extrusion from the DTC ligand (Supporting Information, Figure S1b). Presumably, the extruded elemental sulfur reacts with mCPBA to form sulfate in the reaction mixture, largely diminishing the yield of oxygenated products.

Greater success in obtaining monooxygenated species was achieved using stoichiometric peroxidations of **1** catalyzed by methyltrioxorhenium (MTO) in CH_3OH, Scheme 2.[33−35] These reactions generate mixtures of the oxygenated products monooxygenate S,S-bound **2a**, S,O-bound **2b**, and the

Scheme 2

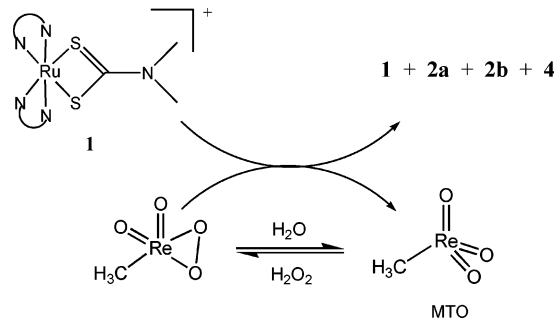

S-extruded monothiocarbamate **4** in 50−70% overall yield, with some black Ru-containing residual that remained on the alumina. Maximum yields were obtained under anaerobic conditions; a typical experiment yielded 10% recovered **1**, 29% **2a**, 8% **2b**, and 17% **4**.

The products were separated by chromatography on a basic alumina column; the observed retention times were inversely proportional to the number of oxygen atoms in each species. Complexes **1** and **2a**,**b** eluted contiguously and required a second column separation to isolate; separate fractions were first analyzed by both UV−vis and ^{1}H NMR before pure fractions were pooled. Complex **2a** was typically the major monooxygenate isolated and was light- and water-sensitive. Complex **2b** was isolated as a minor component but much longer lived in both solution and solid state. The next complex to elute was **4**, which was air-stable but somewhat water-sensitive. Complex **3**, if present, was the last to elute; it was air- and water-stable and highly soluble in protic solvents.

Spectroscopic data on the oxygenated Ru complexes are given in Table 1; samples of UV−vis spectra and IR spectra are given in the Supporting Information (Figures S2 and S3). Electrospray mass spectroscopy obtained the expected parent ions mass/charge unit for the assigned structures; the two monooxygenates obtained the same parent ion mass but different UV−vis and ^{1}H NMR spectra. The IR spectra of **2b** displayed a distinct absorbance at 804 cm^{-1}, on the shoulder of the strong bipyridine peak at 842 cm^{-1}, in the region expected for ν(SO) stretch of *S*,*O*-peroxydithiocarbamates.[25,26] Assigning the ν(SO) absorbance in the spectra of **2a** is more problematic, due to variations between spectra and to sample instability; a tentative assignment at 1030 cm^{-1} is proposed. The IR spectra of **3** displayed bands at 1144 and 1048 cm^{-1} assignable to $\nu_{as}(SO_2)$ and $\nu_s(SO_2)$, respectively, well within the expected range.[17] The IR spectra of **4** are consistent with monodentate monothiocarbamates;[36,37] the ν(CN) and ν(CO) bands are clearly resolved and consistent with the monodentate S-bound form observed in the crystallographic determination.

The complexes **1**−**4** were examined by cyclic voltammetry to determine the effect of S-oxygenation on the $Ru^{III/II}$

(33) Adam, W.; Mitchell, C. M.; Saha-Mollor, C. R. *J. Org. Chem.* **1999**, *64*, 3699−3707.
(34) Espenson, J. H.; Huang, R. *J. Org. Chem.* **1999**, *64*, 6935−6936.
(35) Herrmann, W. A.; Fischer, R. W.; Scherer, W.; Rauch, M. U. *Angew. Chem., Int. Ed. Engl.* **1993**, *32*, 1157−1160.
(36) McCormick, B. J. *Coord. Chem. Rev.* **1984**, *54*, 99−130.
(37) McCormick, B. J.; Stormer, B. P. *Inorg. Chem.* **1972**, *11*, 729−735.

Table 1. Physical and Spectroscopic Properties of **1**−**4** Ruthenium(II) Complexes

param	1	2a	2b	3	4
color	red	purple	red	yellow	brown
ESI (*m*/*z*)	534	550	550	566	518
UV−vis (nm)	294 (38 000)	296 (18 200)	295 (30 700)	284 (40 700)	288 (27 800)
(ϵ, $M^{-1}\,cm^{1}$)[a]	349 (8400)	352 (4500)	348 (7100)	425 (6700)	433 (4000)
	518 (6200)	522 (2900)	502 (4800)		
IR (cm^{-1})[b]		ν(SO) 1030	ν(SO) 804	$\nu_{as}(SO_2)$ 1144	ν(CO) 1604
				$\nu_{s}(SO_2)$ 1048	
$E_{1/2}$ ox[c]	0.607	0.516	0.516	irrev 1.12	0.438

[a] All complexes are dissolved in CH_3CN; spectra given in Supporting Information Figure S2. [b] KBr pellets; spectra given in Supporting Information Figure S3. [c] Oxidation potentials in V vs Ag/AgCl, glassy carbon working electrode, 0.1 M [*n*-Bu_4N][PF_6]/CH_3CN; scan rate = 250 mV/s; Supporting Information Figure S4.

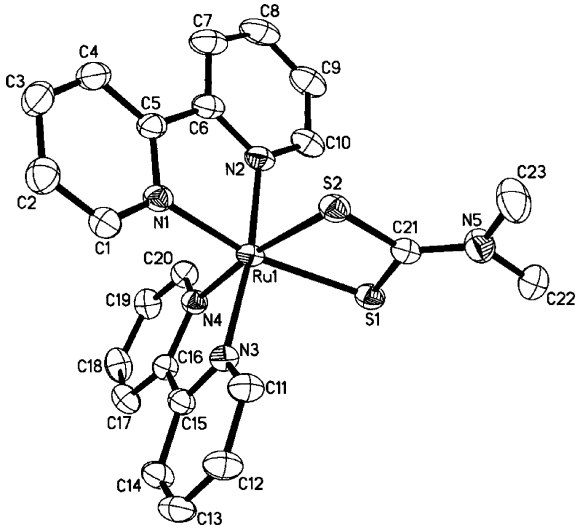

Figure 2. X-ray crystal structure of the molecular cation **1**. Selected bond lengths (Å): Ru(1)−S(1) 2.4069(9); Ru(1)−S(2) 2.3840(9); S(1)−C(21) 1.725(3); S(2)−C(21) 1.721(4); N(5)−C(21) 1.320(5). Selected bond angles (deg): S(1)−Ru(1)−S(2) 73.11(3); C(21)−S(1)−Ru(1) 87.09(12); C(21)−S(2)−Ru(1) 87.91(12); S(2)−C(21)−S(1) 111.82(19); N(5)−C(21)−S(1) 124.2(3); N(5)−C(21)−S(2) 124.0(3); C(21)−N(5)−C(23) 122.1(3); C(21)−N(5)−C(22) 121.8(3); C(23)−N(5)−C(22) 116.1(3).

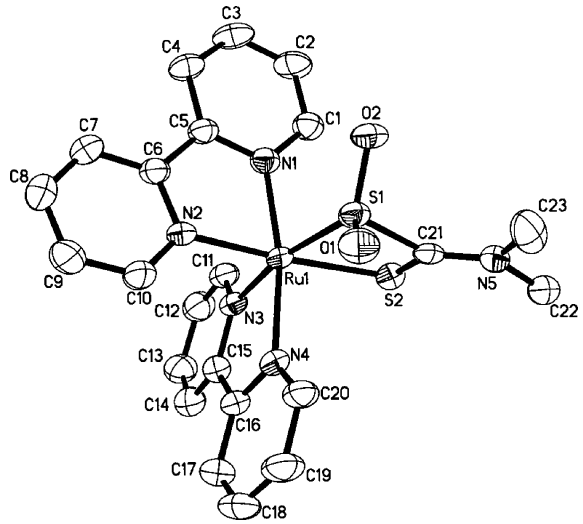

Figure 3. X-ray crystal structure of the molecular cation **3**. Selected bond lengths (Å): Ru(1)−S(1) 2.2497(18); Ru(1)−S(2) 2.3996(18); S(1)−C(21) 1.862(7); S(2)−C(21) 1.698(8); N(5)−C(21) 1.286(9); S(1)−O(1) 1.470-(5); S(1)−O(2) 1.471(5). Selected bond angles (deg): S(1)−Ru(1)−S(2) 74.24(6); C(21)−S(1)−Ru(1) 90.4(2); C(21)−S(2)−Ru(1) 89.6(2); S(2)−C(21)−S(1) 104.1(4); N(5)−C(21)−S(1) 127.4(6); N(5)−C(21)−S(2) 128.5(6); O(1)−S(1)−O(2) 112.4(3); C(21)−N(5)−C(23) 123.4(7); C(21)−N(5)−C(22) 121.0(7); C(23)−N(5)−C(22) 115.5(6).

reduction potential, Supporting Information Figure S4. S-oxygenation may be expected to withdraw electron density from the metal center, thus leading to a more positive reduction potential, as has been previously seen for other series of mono- and dioxygenated metal−thiolate complexes.[38] Contrary to such expectations, the initial monooxygenation lowers the observed reversible reduction potential, i.e., makes the Ru^{III} more stable. Previous examinations of the electrochemical effect of S-oxygenation on the Cr−peroxydithiocarbamate showed surprisingly little effect on the metal-based potential.[39] The mixed effect of S-oxygenation on the metal-based potential is likely because of the highly delocalized bonding within the DTC-derived ligands.

Crystallographically Determined Structures. The structure of **1** was established by X-ray diffraction and is shown in Figure 2; only one of two crystallographically distinct complexes in the unit cell is shown. Characteristic of dithiocarbamates is extensive π delocalization within the S_2-CN moiety, which results in an essentially coplanar geometry; all bond distances are intermediate between the sum of the single bond and double bond radii and fall well within the range seen for previous structures[30] The delocalized interaction extends to Ru; the sum of the 4 angles, Ru−S−C−S′, is 359.93°.

An orange crystal of dioxygenated **3** was obtained by slow solvent diffusion, and its structure was confirmed by X-ray diffraction. Figure 3 shows the distorted octahedral environment for the Ru(II) center, with two N−Ru−S angles at 101.82 and 175.39°, caused by steric interactions with the SO_2 moiety. The coplanar character of S_2CN is maintained, but the C−S bonds are valence localized; the (O_2)S(1)−C(21) bond length, at 1.862(7) Å, is longer as compared to the S(2)−C(21) bond length, at 1.698(8) Å, as well as the shorter S(1)−C(21) bond of the starting material compound **1**, at 1.721(4) Å.

X-ray diffraction analysis of a brown crystal of monothiocarbamate **4** gave the structure seen in Figure 4. A slightly distorted octahedral environment about Ru is seen, with a monodentate MTC, two bidentate bipyridines, and one CH_3CN coordinated from the solvent. The coplanarity of the OSCN atoms implies the delocalization of π electrons is maintained, as with the valence localization apparent in

(38) Farmer, P. J.; Reibenspies, J. H.; Lindahl, P. A.; Darensbourg, M. Y. *J. Am. Chem. Soc.* **1993**, *115*, 4665−74.
(39) Bond, A. M.; Wallace, G. G. *Inorg. Chem.* **1984**, *23*, 1858−1865.

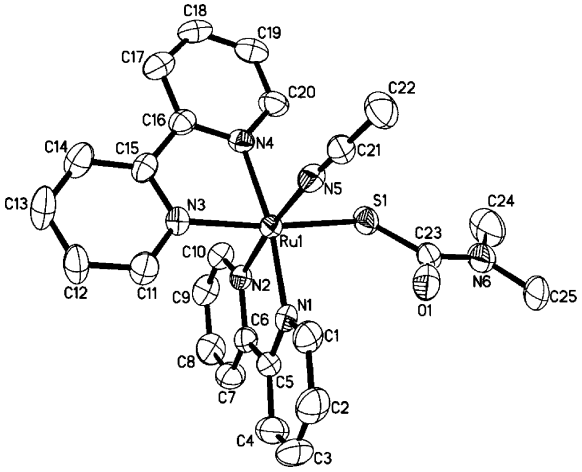

Figure 4. X-ray crystal structure of the molecular cation **4**. Selected bond lengths (Å): Ru(1)−S(1) 2.3761(12); S(1)−C(23) 1.759(6); O(1)−C(23) 1.250(7); N(6)−C(23) 1.365(7). Selected bond angles (deg): N(5)−Ru(1)−S(1) 89.49(11); C(23)−S(1)−Ru(1) 112.4(2); O(1)−C(23)−S(1) 122.9(4); O(1)−C(23)−N(6) 121.1(5); N(6)−C(23)−S(1) 116.0(5); C(23)−N(6)−C(24) 124.8(5); C(23)−N(6)−C(25) 119.6(6); C(24)−N(6)−C(25) 115.6(5).

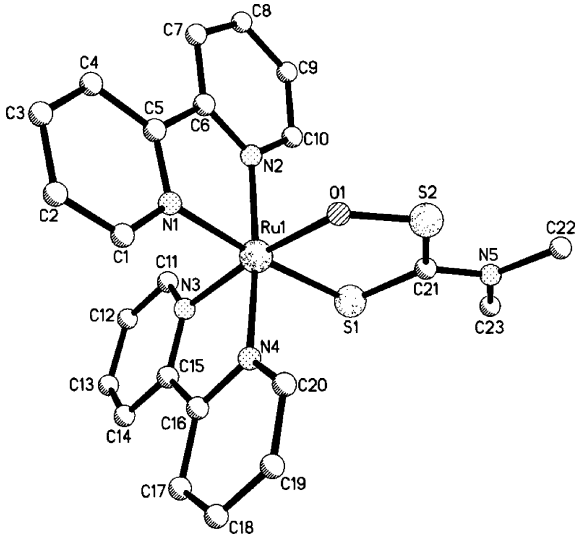

Figure 5. X-ray crystal structure of the molecular cation **2b**, showing connectivity of this regioiosmer of the monooxygenated product.

the single C−S bond (1.759(6) Å) and double C−O bond (1.250(7) Å).

After many attempts, a red crystal of monooxygenate **2b** was isolated by slow solvent diffusion, and Figure 5 shows the structure obtained by X-ray diffraction. The diffraction data were of poor quality, but the analysis confirms the O,S-coordination mode of the peroxydithiocarbamate. The oxygen atom inserts to form a five-member coordinate ring, with the planarity of the ligand largely maintained. Because of the poor quality of the diffraction data, metric values will not be discussed but may be accessed in the Supporting Information.

Structural Considerations. As in the parent compound **1**, there is extensive bond delocalization within all the dithiocarbamate-derived moieties; the planarity of the C_2NCS_2 framework is maintained in all of the complexes structurally characterized, indicating strong π-delocalization despite S-oxygenation or extrusion. The effect of S-based

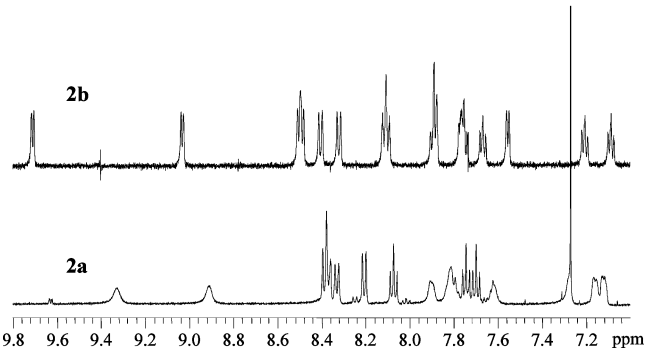

Figure 6. Comparison of the room-temperature ^{1}H NMR spectra of S,O-bound **2b** and S,S-bound **2a**.

derivation may be somewhat quantified by comparison of specific bond lengths. In the parent dithiocarbamate **1**, the C−S bonds of the DTC ligand are similar (1.725(3) and 1.721(4) Å). The bond localization is observed in the dioxygenated **3**, with a lengthening of the C−S bond to the oxygenated sulfur and a shortening of the other (1.862(7) vs 1.698(8) Å), with the single C−S bond in the MTC derivative **4** (1.759(6) Å) being somewhat intermediate. But as noted, both the mono- and dioxygenated sulfurs in **2b** and **3** remain coplanar within the C_2NCS_2 framework.

NMR Characterization. A comparison of NMR spectra of the complexes **1**−**4** is crucial to assigning a structure to monooxygenate **2a**, which could not be crystallized. The ^{1}H NMR spectra of the starting dmDTC complex **1** displayed 8 distinct protons in the aromatic region for the two bipyridine molecules; 16 protons are observed for oxygenated derivatives **2b**, **3**, and **4**. Peak assignments were confirmed by a COSY spectrum (Supporting Information Figure S5−8). Peaks assigned to the two protons closest to the mDTC sulfur atoms are equivalent in **1** (9.64 ppm) but not in the other species and two broad singlets in the spectra for **2a** (9.33 and 8.91 ppm), and into two doublets for **2b** (9.69 and 9.06 ppm), **3** (10.47 and 9.55 ppm), and **4** (9.94 and 9.38 ppm). Likewise, the methyl absorbances are no longer equivalent and observed as two distinct singlets for **3**, but in spectra of **2a**,**b** and **4** the peaks are broadened by thermal exchange due to rotation about the C−N bond of the dmDTC ligand.

An important difference is seen in the room-temperature ^{1}H NMR spectra of the monooxygenates **2a**,**b**, as the former has exchange-broadening evident for several bipyridyl peaks, Figure 6. Variable-temperature ^{1}H NMR spectra of the methyl region of the S,O-bound peroxydithiocarbamate **2b** also display exchange behavior; a singlet corresponding to rapidly exchanging methyl groups at 25 °C gradually split into two singlets at lower temperatures, with coalescence at 258 K, Supporting Information Figure S9. For the S,S-bound monooxygenate **2a**, the methyl peak splits into nonequivalent peaks within a similar temperature range, Figure 7. Exchange-splitting of the protons closest to the mDTC sulfur atoms is also observed, with a greater broadening seen for the upfield proton. Both the methyl and bipyridinyl peaks have equal integration. Likewise, the splitting of the methyl peak is equivalent, implying equal population of the two observed states. This suggests a coupling of the methyl exchange with

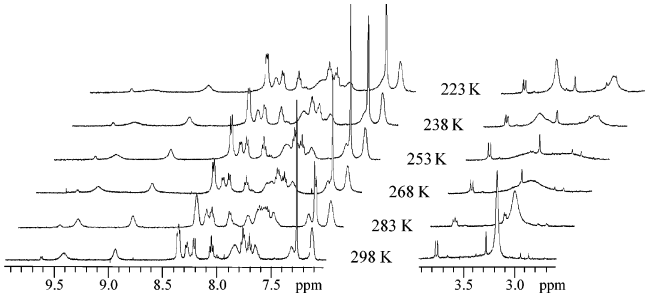

Figure 7. Variable-temperature ^{1}H NMR of S,S-bound **2a** in the bipyridyl and methyl regions.

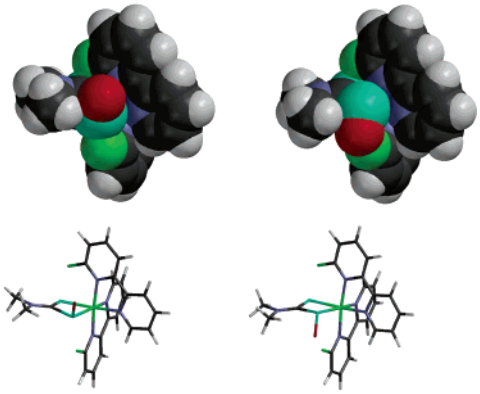

Figure 8. Computer-generated space-filling and tube models of the two Λ diastereomers of Ru(bpy)$_2$(*N*,*N*-dimethylperoxydithiocarbamate-*S*,*S*), **2a**, with *R* stereochemistry at the sulfur on the left. The sulfur atoms are blue, oxygens are red, and the two diastereomeric bipyridyl protons closest to the DTC are colored green for identification.

a second process which we believe is the pyramidal inversion of the chiral sulfenic S atom, a process unique to an S,S-bound monooxygenate. This second process is still rapid at 223 K and thus is significantly more facile than that of the hindered rotation about the C−N bond.

Examination of simple CPK computer-based models of the two Λ diastereomers of an S,S-bound peroxydithiocarbamate complex, Figure 8, shows that the diastereomeric bipyridinyl protons closest to mDTC have distinctly different environments in the two forms. In the up-form, with *S*-stereochemistry at the sulfenyl sulfur, the oxygen is well removed from the bipyridyl protons, with the closest interaction over 4 Å away. The down-form, with *R*-stereochemistry, has very close interactions with two bipyridyl protons at 1.75 and 3.92 Å and another just over 4 Å. Thus, a pyramidal inversion of the sulfur, with the associated movement of the oxygen atom, would explain the observed broadening of bipyridyl protons.

Reactivity of the Monooxygenates. Both monooxygenated complexes were unstable over time and stored as solids in the absence of light. In acetonitrile solution, the S,S-bound **2a** undergoes an apparent intermolecular disproportionation of the sulfenate moiety, yielding the dioxygenate **3** and the deoxygenated **1** over the period of 1 day. The O,S-bound **2b** undergoes a slower decomposition in solution but yields no identifiable Ru-containing products. Solutions of **2a**, when treated with stoichiometric mCPBA, gave the dioxygenate **3** in good yield. Exposure to air or oxygen gas leads to decomposition, with the S-extruded deriviative **4** generated in low yeild.

O-atom-transfer disproportionation has been previously observed for Ni-bound sulfenate complexes but was initiated by electrochemical reduction or oxidation.[13] To test the O-atom-transfer ability of **2a**, a sample was reacted with a 10-fold excess of PEt_3 in an airtight NMR tube and the reaction followed by ^{31}P and ^{1}H NMR. After completion, the ^{31}P NMR showed a new peak corresponding to $OPEt_3$, and the ^{1}H NMR spectra showed complex **1** as the only Ru complex. (Supporting Information Figure S11).

Mechanistic Considerations. The intent of this work was to isolate the initial products of S-oxygenation of a substitutionally inert metal-bound DTC and structurally characterize their subsequent transformations. The reactivity observed is summarized with the isolated products in Scheme 3. As expected, initial peroxygenation gives a monooxygenated product; the major form **2a** is tentatively assigned as a diastereomeric mixture of isomers of the S,S-bound peroxydithiocarbamate. This species is highly reactive and is the apparent precursor to the S,S-bound dioxygenate **3** and S-extruded product **4**. The dioxygenate **3** is to our knowledge the first characterized example of an S,S-bound thiocarbamate−sulfinate, and the monothiocarbate adduct **4** is the first produced via S-extrusion of a metal-bound dithiocarbamate. Both structures validate our belief that the slow ligand exchange from the Ru(bpy)$_2^{2+}$ moiety would allow isolation of DTC-derived species.

The solvent is seen to play a significant role in determining the observed products of S-oxygenation. As has been

Scheme 3 [a]

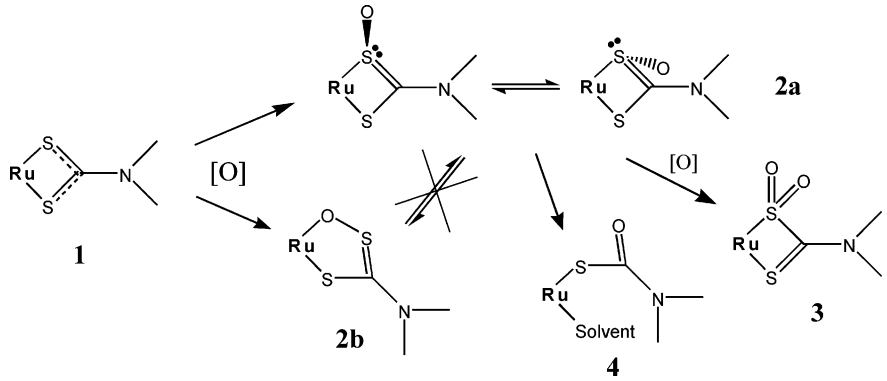

[a] Ru = Ru(bpy)$_2^{2+}$.

previously noted in the oxygenation of Ni−thiolates,[13] reactions run in CH_3OH have the highest yield of monooxygenated products. Hydrogen bonding likely stabilizes the S-oxygenated products, and the effect of such interactions were observable electrochemically in a series of Ni−thiolate complexes.[38] In this case, nonprotic solvents such as $CHCl_3$ or CH_2Cl_2 promote the further reactivity of the monooxygenate **2a**, increasing the isolable yields of both the dioxygenate **3** and S-extruded product **4**.

Less expected was the facile interconversion of the diastereometric pair of the monooxygenates **2a**, apparently via pyramidal inversion of the Ru-bound sulfur. Although we were unable to freeze out this process, the observed line-broadening in the NMR spectra of **2a** at low temperature suggests that the activation barrier is quite low. A reviewer has noted that electronegative substituents typically slow the rate of sulfur atom inversion.[40] But conjugation of the sulfur to unsaturated systems results in greatly increased S-inversion, both in aryl and allylic sulfoxides[41] and metal complexes of dialkyl sulfides.[42] Thus the extended delocalization of the dithiocarbamate backbone may facilitate S-inversion.

One pathway for such an racemization would be via a linkage isomerization from S,S-bound to S,O-bound.[41] But the S,O-bound isomer, **2b**, is isolable from **2a**, and no interconversion between the two forms was observed. The formation of the two linkage isomers **2a**,**b** must therefore be via separate pathways which are as yet poorly defined. The two previously characterized peroxydithiocabamate complexes were both S,O-bound,[25,29] perhaps due to the apparent greater inherent stability of this adduct. In this work, the S,O-bound form was a very minor product isolable only in reactions catalyzed by MTO.

Several key questions remain from this initial work. First, what differentiates the formation and stabilities of the S,S- and S,O-bound linkage isomers of a peroxydithiocarbamate complex? Second, how might metal−DTC interactions distinguish between these two paths of S-oxygenation? Further, by what mechanism does the S-extrusion occur and what are the S-based byproducts? Efforts are underway to address these points.

Experimental Section

Materials. All common laboratory solvents were reagent grade. Solvents in the nitrogen glovebox were dried using standard techniques. *cis*-Dichlorobis(2,2′-bipyridine)ruthenium(II) dihydrate, 99%, was purchased from Strem Chemicals. Basic alumina was purchased from Fisher Scientific, and all other chemicals were purchased from Aldrich Chemical Co. and used as obtained. Unless otherwise noted, manipulations were carried out using standard Schlenk techniques and a nitrogen dry glovebox to maintain anaerobic conditions during synthesis. Isolation of products was carried out in air, except **2b**.

Physical Measurements. Mass spectra were determined by Micromass LCT. UV−vis spectra were recorded by a Perkin-Elmer Lambda 900. ^{1}H and ^{31}P NMR spectra were recorded using Bruker Avance 400 and 500 MHz spectrometers. Chemical shifts are referenced via the solvent signal. Infrared spectra were recorded as KBr pellets on an Impact 410 from Nicolet. Elemental analyses were performed by Atlantic Microlab, Norcross, GA. Cyclic voltammetry was performed using a Bio-Analytical Systems 100B electrochemical analyzer with a glassy carbon stationary electrode and a platinum wire electrode. Samples were recorded in CH_3CN solution with 100 mM $(TBA)PF_6$ as the supporting electrolyte, with an Ag/AgCl reference electrode. All single-crystal X-ray diffraction structures were solved at the X-ray Crystallography Facility at UCI.

Syntheses. All reactions were performed under nitrogen inert atmosphere using Schlenk techniques or a glovebox, except the preparation of **1.** All of the monocationic ruthenium complexes were purified and separated by basic alumina chromatography (Brockman activity I, 60−325 mesh, Fisher) using mixtures of CH_2Cl_2, CH_3CN, and CH_3OH.

Preparation of Ru(bpy)$_2$(*N*,*N*-dimethyldithiocarbamate)(PF$_6$), 1. To a solution of *cis*-dichloro(2,2-bpy)Ru^{II} (1.22 g, 2.52 mmol) in ethylene glycol (60.0 mL) was added sodium dimethyldithiocarbamate hydrate (0.411 g, 2.87 mmol). The mixture was heated at 110 °C for 5 min. Water (50.0 mL) was added to the mixture, followed by excess of KPF_6. The precipitates were collected by vacuum filtration, and the air-stable product was recrystallized from CH_3CN/Et_2O (yield: 1.53 g, 89.5%). Slow diffusion crystallization yielded a blackish red rectangular crystal utilized in the diffraction studies. ESI/MS: *m*/*z* 534. UV−vis (nm): 294, 349, 518. ^{1}H NMR (500 MHz, $CDCl_3$): δ 9.63 (d, 2H), 8.36 (d, 2H), 8.24 (d, 2H), 8.03 (t, 2H), 7.73 (t, 2H), 7.64 (t, 2H), 7.64 (d, 2H), 7.13 (t, 2H), 3.29 (s, 6H). Anal. Calcd for $RuN_5S_2C_{23}H_{22}PF_6$: C, 40.7; H, 3.28; N 10.3. Found: C, 40.4; H, 3.49; N, 10.3.

Preparation of Ru(bpy)$_2$(*N*,*N*-dimethylthiocarbamatesulfinate-*S*,*S*)$^+$, 3. To a solution of **1** (0.0868 g, 0.12 8 mmol) in 250 mL of degassed CH_3CN was added a 100-fold excess of 30% H_2O_2 (1.3 mL, 0.0126 mol), which was allowed to react over 1 day, during which the color of the solution changed from darkish red to orange. DMS (10 mL, 0.136 mol) was added, and the mixture was stirred overnight to neutralize the excess peroxide. The bright orange product was evaporated to a 10 mL solution in DMSO, which was then dried under high vacuum. The resulting solid **3** was purified on a basic alumina column by elution with CH_2Cl_2/CH_3CN (50/50 v/v) (yield: 86%). The purified **3** was recrystallized from CH_3CN/petroleum ether by slow diffusion giving a rectangular orange crystal for diffraction studies. ESI/MS: *m*/*z* 566. UV−vis (nm): 284, 425. ^{1}H NMR (500 MHz, CD_3OD): δ 10.47 (d, 1H), 9.55 (d, 1H), 8.66 (d, 1H), 8.64 (d, 1H), 8.59 (d, 1H), 8.51 (d, 1H), 8.29 (t, 1H), 8.23 (t, 1H), 8.04 (t, 1H), 7.96 (t, 1H), 7.84 (m, 2H), 7.75 (d, 1H), 7.65 (d, 1H), 7.39 (t, 1H), 7.30 (t, 1H), 3.57 (s, 3H) 3.29 (s, 3H). IR (cm^{-1}): 1143 ($\nu_{as}SO_2$) and 1049 (ν_sSO_2). Anal. Calcd for $RuN_5S_2C_{23}H_{22}O_2PF_6{\cdot}CH_2Cl_2$: C, 36.72; H, 3.10; N 8.61. Found: C, 36.23; H, 3.04; N, 8.80.

Generation and Isolation of Ru(bpy)$_2$(*N*,*N*-dimethylperoxydithiocabamate-*S*,*S*)$^+$, 2a, Ru(bpy)$_2$(*N*,*N*-dimethylperoxydithiocabamate-*O*,*S*)$^+$, 2b, and Ru(bpy)$_2$(dimethylmonothiocarbamate)$^+$, 4. A degassed solution of **1** (0.108 g, 0.127 mmol) in 300 mL of CH_3OH containing 0.1 M triflic acid (2.6 mL) and 0.01 mmol (0.0031 g) of methyltrioxorhenium (MTO) was stirred at room temperature at dark for 15 min, followed by the addition of 1 equiv of 30% H_2O_2 (24 μL). When the color changed from darkish red to brownish orange in 30 min, an excess of $NaHCO_3$ (approximately 0.5 g) was added to the mixture to stop the reaction. The solution

(40) Abel, E. W.; Bhargava, S. K.; Kite, K.; Orrell, K. G.; Sik, V.; Williams, B. L. *Polyhedron* **1982**, *1*, 289−298.
(41) Bickart, P.; Carson, F. W.; Jacobus, J.; Miller, E. G.; Mislo, K. *J. Am. Chem. Soc.* **1968**, *90*, 4869−4876.
(42) Abel, E. W.; Moss, I.; Orrell, K. G.; Sik, V. J. *Organomet. Chem.* **1987**, *326*, 187−200.

was evaporated to dryness by rotor-vaporization and the solid dissolved in CH_2Cl_2 and washed with DI water three times. The product compounds were separated on a basic alumina column by elution with CH_2Cl_2 and adding increasing aliquots of CH_3CN; compounds were collected in the order of hydrophobicity. Isolated yields from a typical reaction: recovered **1** (5%) and then **2a** (29%), **2b** (8%), and **4** (17%); some unidentified colored product remained on the column.

The two different forms of **2** were separated on a second alumina column, with identical ESI-MS but different ^{1}H NMR and UV−vis spectra. The O,S-bound form **2b** was recrystallized from CH_3CN/diethyl ether by slow diffusion giving a rectangular red crystal for diffraction studies. All attempts at crystallization of **2a** have been unsuccessful. ESI/MS: *m*/*z* 550 (**2a**,**b**). UV−vis (nm): **2a**, 352, 465, 522; **2b**, 348, 464, 502. ^{1}H NMR of **2a** (500 MHz, CD_3Cl): δ 9.33 (bs, 1H), 8.91 (bs, 1H), 8.38 (t, 2H), 8.34 (d, 1H), 8.22 (d, 1H), 8.07 (t, 1H), 7.90 (bs, 1H), 7.81 (bs, 3H), 7.75 (t, 1H), 7.70 (t, 1H), 7.62 (bs, 1H), 7.16 (bs, 1H), 7.12 (bs, 1H), 3.18 (bs, 6H). ^{1}H NMR of **2b** (500 MHz, CD_3Cl): δ 9.69 (d, 1H), 9.06 (d, 1H), 8.51 (d, 1H), 8.43 (d, 1H), 8.34 (t, 2H), 8.07 (q, 2H), 7.83 (t, 1H), 7.75 (d, 2H), 7.64 (m, 2H), 7.46 (d, 1H), 7.19 (t, 1H), 7.08 (t, 1H), 3.25 (bs, 6H). IR (ν(SO), cm^{-1}): **2a**, 1030; **2b**, 803 cm^{-1}. Anal. Calcd for $RuN_5S_2C_{23}H_{22}OPF_6 \cdot 1.5CH_3OH$: C, 38.81; H, 3.50; N 9.43. Found: C, 38.78; H, 3.52; N, 9.04.

Complex **4** was isolated from the above reaction; a purified sample was recrystallized from CH_3CN/diethyl ether by slow diffusion giving a rectangular red crystal for diffraction studies. EI/MS: *m*/*z* 518 (M^+, 100). UV−vis (nm): 288, 433. ^{1}H NMR (500 MHz, CD_3CN): δ 9.94 (d, 1H), 9.38 (d, 1H), 8.43 (d, 1H), 8.36 (d, 1H), 8.32 (d, 1H), 8.21 (d, 1H), 8.14 (t, 1H), 8.03 (t, 1H), 7.84 (t, 1H), 7.73 (m, 2H), 7.63 (t, 2H), 7.56 (d, 1H), 7.21 (t, 1H), 7.04 (t, 1H), 3.57 (bs, 6H). IR (cm^{-1}): 1560 (ν(CN)), 1604 (ν(CO)). Anal. Calcd for $RuN_5SC_{23}H_{22}OPF_6 \cdot CH_3CN \cdot 3H_2O$: C, 39.7; H, 4.09; N 11.09. Found: C, 39.86; H, 3.39; N, 10.80.

Acidic Peroxidations. To an aerobic solution of **1** (0.0118 g, 0.174 mmol) in 20 mL of CH_3OH were added a few drops of 2 N HCl to acidify the solution to ca. pH 4. Then, 1 equiv of mCPBA was added at 0 °C. The color immediately changed from red to yellow; complex **3** was the major product as detected by ESI/MS.

Anaerobically, to a solution of **1** (0.0229 g, 0.337 mmol) in 100 mL of CH_3OH and 0.1 M HOTf, 1 equiv of H_2O_2 was added to the mixture at room temperature. The color of the reaction mixture changed over 10 min from red to yellow; complex **3** was the major product as detected by ESI/MS. Purification by basic alumina gave a 20% recovered yield.

Reaction of 1 with Stoichiometric mCPBA. A solution of **1** (0.0256 g, 0.0377 mmol) in 100 mL of CH_2Cl_2 was stirred at 0 °C, followed by dropwise solution of 77% mCPBA (0.0132 g, 0.0589 mmol) in 10 mL of CH_2Cl_2. An excess of $NaHCO_3$ was added to the mixture, which was stirred at low-temperature overnight. The ESI/MS in situ showed ca. 5% **2** was formed. Attempts to isolate any oxygenated products by column chromatography were unsuccessful. The main product eluted from the column was complex **1**.

Protic vs Aprotic Solvent. Complex **1** (0.101 g, 0.148 mmol) was dissolved in 200 mL of CH_3OH and cooled for 1 h in a heavily salted ice water bath, and then 1.1 equiv of mCPBA (0.0356 g, 0.159 mmol) was added slowly to the mixture aerobically dropwise with constant stirring over a 10 min period. The monooxygenated product **2** was detected by ESI/MS, in a less than 10% yield.

Complex **1** (0.1028, 0.151 mmol) was dissolved in 200 mL of CH_3CN and cooled for 1 h in a heavily salted ice water bath, and then 1.1 equiv of mCPBA (0.0372 g, 0.166 mmol) was added slowly to the mixture aerobically dropwise with constant stirring over 10 min period. The dioxygenated and S-extruded products **3** and **4** were detected by ESI/MS, both totaling less than 10%.

Reaction of 1 with Other Oxygenating Agents. A solution of **1** (0.0340 g, 0.0501 mmol) in 200 mL of CH_3CN was stirred at room temperature, followed by an excess of oxone (0.10 g, 0.163 mmol). The color changed from red to orange over 3 h. The excess of oxone was then filtered by vacuum filtration, followed by column chromatography separation, yielding 60−70% of complex **3**.

To a solution of **1** (0.0048 g, 0.0071 mmol) in 10 mL of CH_3CN was added 1 equiv of Ag_2O (0.0030 g, 0.0129 mmol), which was stirred for 1 h at room temperature. ESI/MS and column chromatography showed that no oxygenation occurred.

To a solution of **1** (0.0050 g, 0.00736 mmol) in 10 mL of CH_3CN was added an excess of NaOCl (23 μL, 0.374 mmol), which was stirred for 1 hour at room temperature. ESI/MS and column chromatography showed that no oxygenation occurred.

O-Atom-Transfer Reactions of 2a. In a glovebox, a sample of **2a** (5.2 mg, 0.0075 mmol) was dissolved in 5 mL of CH_3CN and kept stirring overnight. After 24 h, the products were separated in a basic alumina chromatography. The yields were 53% for **1** and 30% for **3**. To confirm O-atom-transfer reactivity, a sample of **2a** (5.4 mg, 0.0078 mmol) was dissolved in $CDCl_3$ in an airtight NMR tube, and a 2-fold excess of PEt_3 (2.4 μL) was added anaerobically. The reaction went to completion as followed by ^{31}P and ^{1}H NMR, giving stoichiometric $OPEt_3$ and **1** as the only Ru-based product. After completion, 61% of **1** was recovered following column separation.

X-ray Data Collection, Structure Solution, and Refinement for 1. A dark red crystal of approximate dimensions 0.21 × 0.22 × 0.28 mm was mounted on a glass fiber and transferred to a Bruker CCD platform diffractometer. The SMART[1] program package was used to determine the unit-cell parameters and for data collection (25 s/frame scan time for a sphere of diffraction data). The raw frame data was processed using SAINT[2] and SADABS[3] to yield the reflection data file. Subsequent calculations were carried out using the SHELXTL[4] program. There were no systematic absences nor any diffraction symmetry other than the Friedel condition. The centrosymmetric triclinic space group $P\bar{1}$ was assigned and later determined to be correct. The structure was solved by direct methods and refined on F^2 by full-matrix least-squares techniques. The analytical scattering factors[5] for neutral atoms were used throughout the analysis. There were two molecules of the formula unit present. In addition there was 3/4 of a molecule of Et_2O solvent present per formula unit (1.5 molecules total). One of the solvent molecules was in a general position while the other was located about an inversion center and was disordered. The disordered atoms were assigned partial site occupancy factors. The hydrogen atoms associated with the disordered solvent molecule were not included in the refinement. The remaining hydrogen atoms were included using a riding model. The fluorine atoms attached to P(2) were disordered and included using multiple components with partial site occupancy factors (0.50 each). At convergence, wR2 = 0.1150 and Goof = 1.027 for 772 variables refined against 14 179 data. As a comparison for refinement on *F*, R1 = 0.0456 for those 11 280 data with $I > 2.0\sigma(I)$.

X-ray Data Collection, Structure Solution, and Refinement for 3. An orange crystal of approximate dimensions 0.14 × 0.16 × 0.20 mm was mounted on a glass fiber and transferred to a Bruker CCD platform diffractometer. The SMART[1] program package was used to determine the unit-cell parameters and for data collection (25 s/frame scan time for a sphere of diffraction data). The raw frame data was processed using SAINT[2] and SADABS[3] to yield the reflection data file. Subsequent calculations were carried out

using the SHELXTL[4] program. There were no systematic absences nor any diffraction symmetry other than the Friedel condition. The centrosymmetric triclinic space group $P\bar{1}$ was assigned and later determined to be correct. The structure was solved by direct methods and refined on F^2 by full-matrix least-squares techniques. The analytical scattering factors[5] for neutral atoms were used throughout the analysis. Hydrogen atoms were included using a riding model. At convergence, wR2 = 0.2028 and Goof = 1.173 for 362 variables refined against 5530 data (0.85 Å resolution). As a comparison for refinement on *F*, R1 = 0.0612 for those 4385 data with $I > 2.0\sigma(I)$.

X-ray Data Collection, Structure Solution, and Refinement for 4. A red crystal of approximate dimensions 0.12 × 0.13 × 0.27 mm was mounted on a glass fiber and transferred to a Bruker CCD platform diffractometer. The SMART[1] program package was used to determine the unit-cell parameters and for data collection (20 s/frame scan time for a sphere of diffraction data). The raw frame data was processed using SAINT[2] and SADABS[3] to yield the reflection data file. Subsequent calculations were carried out using the SHELXTL[4] program. The diffraction symmetry was 2/*m*, and the systematic absences were consistent with the centrosymmetric monoclinic space group $P2_1/c$, which was later determined to be correct. The structure was solved by direct methods and refined on F^2 by full-matrix least-squares techniques. The analytical scattering factors[5] for neutral atoms were used throughout the analysis. Hydrogen atoms were included using a riding model. There were two molecules of the formula unit present. There was also a half-molecule of acetonitrile present/formula unit. The fluorine atoms associated with P(2) were disordered and included using multiple components (0.70/0.30) with partial site occupancy factors. At convergence, wR2 = 0.1186 and Goof = 1.027 for 748 variables refined against 11 526 data (0.80 Å). As a comparison for refinement on *F*, R1 = 0.0436 for those 8259 data with $I > 2.0\sigma(I)$.

X-ray Data Collection, Structure Solution, and Refinement for 2b. A red crystal of approximate dimensions 0.14 × 0.20 × 0.22 mm was mounted on a glass fiber and transferred to a Bruker CCD platform diffractometer. The SMART[1] program package was used to determine the unit-cell parameters and for data collection (25 s/frame scan time for a sphere of diffraction data). The raw frame data was processed using SAINT[2] and SADABS[3] to yield the reflection data file. Subsequent calculations were carried out using the SHELXTL[4] program. There were no systematic absences nor any diffraction symmetry other than the Friedel condition. The centrosymmetric triclinic space group $P\bar{1}$ was assigned and later determined to be correct. The structure was solved by direct methods and refined on F^2 by full-matrix least-squares techniques. The analytical scattering factors[5] for neutral atoms were used throughout the analysis. Hydrogen atoms were included using a riding model. There were two molecules of the formula unit present. There was also one-quarter molecule of diethyl ether solvent present/formula unit. The solvent was disordered and included using multiple components with partial site occupancy factors. Final least-squares refinement yielded wR2 = 0.2636 and Goof = 1.071 for 498 variables refined against 8155 data (0.90 Å data cutoff). As a comparison for refinement on *F*, R1 = 0.0897 for those 4973 data with $I > 2.0\sigma(I)$. Due to the poor data quality it was necessary to refine all carbon atoms using isotropic thermal parameters.

Computer Modeling. The computer-generated models of the four diastereomers of peroxydithiocabamate **2a** were generated using the Spartan Semiempirical Program 5.0, and the geometry optimizations were performed at the PM3 level.

Acknowledgment. We thank Professor James Nowick for his assistance with the analysis of variable-temperature NMR. This research is supported by the Petroleum Research Foundation (Grant CHE-0100774 to P.J.F.).

Supporting Information Available: ESI-MS analysis of oxygenation reactions and further characterizations of compounds **1**−**4** including electronic and IR absorbance spectra, cyclic voltammograms, 2D ^{1}H NMR spectra, and crystallographic data in CIF format. This material is available free of charge via the Internet at http://pubs.acs.org.

IC048661A